Published in final edited form as:
Oncogene. 2010 January 21; 29(3): 335–344. doi:10.1038/onc.2009.333.

Activated BRAF induces gliomas in mice when combined with *Ink4a/Arf* loss or Akt activation

James P. Robinson, Ph.D[1], **Matthew W. VanBrocklin, Ph.D**[1], **Adam R. Guilbeault, BS**[1], **Denise L. Signorelli, Ph.D**[1], **Sebastian Brandner, M.D.**[2], and **Sheri L. Holmen, Ph.D**[1]

[1] Drug Development Department, Nevada Cancer Institute, Las Vegas, NV, 89135, USA

[2] Division of Neuropathology, UCL Institute of Neurology, London, WC1N 3BG, UK

Abstract

Mutations in receptor tyrosine kinase (RTK) growth factor receptors (*EGFR, PDGFR, MET* and *ERBB2)*, which result in downstream activation of the RAS/RAF/MEK/ERK mitogen-activated protein kinase (MAPK) pathway and PI(3)K/AKT pathway, are found in almost all high grade gliomas and MAPK signaling is necessary for continued glioma maintenance. In addition, BRAF is mutated in the majority of low grade gliomas and its expression and activity is significantly increased in the majority of high grade gliomas. While the importance of RTKs and RAS signaling in glioma development has been demonstrated, the role of BRAF has yet to be characterized. We evaluated the effect of activated BRAF in glioma formation using the retroviral RCAS/TVA system to transfer genes encoding activated forms of BRAF, KRas, Akt and Cre to Nestin expressing neural progenitor cells in *Ink4a/Arf* $^{lox/lox}$ mice *in vivo*. While expression of activated BRAF alone is not sufficient for tumorigenesis, the combination of activated BRAF and Akt or BRAF with *Ink4a/Arf* loss is transforming. Interestingly, activated BRAF generates gliomas with characteristics similar to activated KRas in the context of Akt but not *Ink4a/Arf* loss. Our studies demonstrate a role for BRAF activation and signaling in glioma development and as potential target for glioma therapy.

Keywords

Glioma; *BRAF*; *KRas*; *AKT*; *Ink4a*; *Arf*

Introduction

Gliomas are named according to the type of cell they most closely resemble (Hill *et al.*, 1999) and sub-categorized according to their grade by the World Health Organization (WHO) (Louis *et al.*, 2007). Recently, a novel *BRAF-KIAA1549* fusion gene was discovered in 66% of pilocytic astrocytomas (PA; WHO grade I) and *BRAF*^{V600E} mutations were found

Correspondence should be addressed to: Sheri L. Holmen, Nevada Cancer Institute, One Breakthrough Way, Las Vegas, NV 89135 (sholmen@nvcancer.org) phone 702-822-5295, fax 702-944-0473..

Conflict of interest
The authors declare no conflict of interest

Supplementary Information is available on the Oncogene website (http://www.nature.com/onc)

in 2% of PAs (Jones *et al.*, 2008). *BRAF*^{V600E} mutations have also been identified in 6% of glioblastoma multiforme (GBM), the highest-grade of glioma (WHO Grade IV) (Basto *et al.*, 2005), and in 11% of glioma cell lines (Davies *et al.*, 2002). In addition, a recent study demonstrated a 5-fold increase in RAF serine/threonine kinase activity in a significant series of GBM coupled with a 12-fold increase in BRAF and a 2-fold increase in CRAF protein levels (Lyustikman *et al.*, 2008). Consistent with these findings, copy number gains including the BRAF locus, 7q35, occur in as many as 63% of anaplastic astrocytomas (Grade III) and grade IV tumors (Jeuken *et al.*, 2007). However, the role of BRAF activation in glioma formation has not yet been evaluated.

Due to alternative splicing and differential usage of at least two initiating codons, both mouse and human *BRAF* genes can encode as many as ten different BRAF protein isoforms with molecular weights ranging from 65 to 105 kDa. However, in neural tissues, the predominant forms are of higher molecular weight (Barnier *et al.*, 1995). This is also the case in human GBM tissue (Lyustikman *et al.*, 2008). Inactivating mutations in the AKT signaling repressor phosphatase and tensin homolog deleted on chromosome ten (*PTEN)* are also common and occur in over 70% of grade IV tumors. In the absence of *PTEN*, AKT activity is elevated leading to increased proliferation and inhibition of apoptosis. AKT activation has also been documented in GBM as a result of increased phosphatidylinositol 3-kinase (PI3K) activity due to mutations within the regulatory subunit of PI3K (PIK3CA) (Mizoguchi *et al.*, 2004). Mutations that inactivate both the pRB and p53 pathways are found in 78% and 87% of Grade IV tumors, respectively (e.g., *MDM2, CCND2, CDKN2C, CDK6, CDKN2A, CDK4, RB* and *TP53*) (Furnari *et al.*, 2007). The *CDKN2A* locus encodes two protein products, INK4a and ARF. INK4a blocks pRb phosphorylation and prevents progression from G_1 to S in the cell cycle while ARF is involved in the regulation of p53 levels (Chin *et al.*, 1998; Roussel, 1999) and acts to arrest the cell cycle in G1 and G2 in response to oncogenic stimuli (Quelle *et al.*, 1995). Mutations in receptor tyrosine kinase (RTK) growth factor receptors *(EGFR, PDGFR, MET* and *ERBB2*) resulting in constitutive downstream signaling of the canonical mitogen activated protein kinase (MAPK) (e.g., RAS/RAF/MEK/ERK) and PI3K/AKT pathways are found in almost all astrocytic tumors.

We and others have used a somatic cell gene delivery method based on the RCAS/TVA system to induce gliomas in mice that express the TVA receptor under control of the Nestin promoter (N-TVA) (Holland *et al.*, 2000; Holmen and Williams, 2005). Combined expression of mutant KRas with either Akt activation or deletion of the *Ink4a/Arf* locus in Nestin expressing neural progenitor cells leads to the development of GBM in mice (Holland *et al.*, 2000; Uhrbom *et al.*, 2002). Mutations in *CRAF*, also known as *RAF-1*, are largely restricted to leukemia's; however, a novel *CRAF* fusion gene was recently identified in 2% of PA (Jones *et al.*, 2009) and activated CRAF can substitute for KRas in combination with Akt activation or *Arf* loss to induce GBM in mice (Lyustikman *et al.*, 2008).

In this study, we used the RCAS/TVA model to assess the role of activated BRAF in glioma development *in vivo*. We show that while *BRAF*^{V600E} is not tumorigenic on its own, cooperation with *Ink4a/Arf* loss or activation of Akt leads to the formation of gliomas in this model. The BRAF^{V600E}/Akt tumors resembled KRas^{G12D} Akt tumors in their histological appearance, incidence, and lethality. In contrast, BRAF^{V600E} and KRas^{G12D} induced tumors

differed significantly in the context of *Ink4a/Arf*-deficiency. These results demonstrate that BRAF plays a role in glioma formation that is context dependent. Due to the high incidence of *BRAF* mutations in low-grade gliomas (Jones *et al.*, 2008; Pfister *et al.*, 2008), overexpression and mutation of BRAF in high grade gliomas (Basto *et al.*, 2005; Jeuken *et al.*, 2007), and the importance of the RAS/MAPK pathway in glioma maintenance (Holmen and Williams, 2005), our findings suggest that BRAF may be a relevant target for therapy in the majority of glioma patients.

Results

Confirmation of stable gene delivery into cultured astrocytes

Astrocytes were isolated from N-TVA/*Ink4a/Arf* $^{lox/lox}$ mice, established in culture and infected with an RCASBP(A) virus encoding *Cre* to delete the *Ink4a/Arf* locus (Supplementary Figure 1). Following loss of *Ink4a/Arf*, these cells proliferated continuously and never experienced a detectable senescence crisis even after 30 population doublings, suggesting they are immortal. This is consistent with the behavior of astrocytes isolated from glial fibrillary acidic protein (GFAP)-TVA mice that had been crossed to mice that are germline deficient for *Ink4a/Arf* (Holland *et al.*, 1998b). The immortal astrocytes were used to evaluate expression and activity of *KRas*^{G12D}*, Akt, and BRAF*^{V600E} (isoform B1) alone and in combination. BRAF isoform B1 contains exons 1-18 but does not contain exons 8b or 9b, which have opposing effects on transformation (Hmitou I. et al., 2007). Delivery and expression of BRAF^{V600E} in astrocytes in culture by infection with RCASBP(A)*BRAF*^{V600E} was observed to be at a similar level and molecular weight to that seen in human GBM cells lines (Supplementary Figure 2). The efficiency of RCASBP(A) infection in N-TVA astrocytes was assessed using RCASBP(A)GFP (Figure 1a). Nearly all of the cells expressed GFP indicating productive infection. Western blot analysis of cell lysates demonstrated viral KRas^{G12D}, BRAF^{V600E} and Akt expression in infected astrocytes (Figure 1b). To ensure that RCASBP(A)*BRAF*^{V600E} and RCASBP(A)*KRas*^{G12D} were both active, we evaluated the levels of phoshporylated ERK 1/2 (P-ERK) following serum starvation. Both constructs induced similar levels of P-ERK indicating that they were equally active. As a consequence of the negative regulatory effects of Akt on BRAF, less P-ERK was observed in RCASBP(A)*BRAF*^{V600E} infected cells that were also infected with RCASBP(A)*Akt* (Figure 1b). The levels of total ERK remained unchanged between the different conditions.

KRas or BRAF activation induces anchorage-independent growth of astrocytes in vitro when combined with Ink4a/Arf loss or Akt activation

The ability of the mutant Ras and BRAF to induce anchorage-independent growth of astrocytes was initially assayed *in vitro* by colony formation in soft agar. Whereas RCASBP(A)Cre or RCASBP(A)GFP infected astrocytes were unable to grow in soft agar, *Ink4a/Arf*-deficient astrocytes expressing activated KRas^{G12D} or BRAF^{V600E} formed numerous colonies in soft agar, demonstrating that activation of this pathway in astrocytes results in anchorage-independent growth, a characteristic of transformed cells. *Ink4a/Arf* wildtype astrocytes infected with RCASBP(A)Akt alone did not form colonies in soft agar but co-expression with activated KRas^{G12D} or BRAF^{V600E} induced anchorage-independent

growth demonstrating the ability of these oncogenes to cooperate with Akt activation or *Ink4a/Arf* loss *in vitro* (Supplementary Figure 3).

Activated BRAF induces gliomas in mice when combined with Ink4a/Arf loss or Akt activation

Following intracranial infection of N-TVA/*Ink4a/Arf* $^{lox/lox}$ mice with various RCASBP(A) viruses, tumor incidence and tumor-free survival was assessed for 14 weeks. All of the mice infected with KRas^{G12D} and Cre viruses developed tumors (17/17), in contrast only 39% (10/26) of the mice injected with BRAF^{V600E} and Cre viruses developed tumors. Tumor incidence was not significantly different between mice infected with KRas^{G12D} or BRAF^{V600E} and Akt with 48% (24/50) of mice infected with KRas^{G12D} and Akt developing tumors compared with 54% (15/28) of mice infected with BRAF^{V600E} and Akt (Figure 1c). It has previously been established that infection with RCASBP(A) KRas^{G12D} or Akt alone is insufficient for tumorigenesis in N-Tva mice (Holland *et al.*, 2000). No mice infected with BRAF^{V600E} (0/28) or Cre (0/10) alone developed tumors. In addition, there is no significant incidence of brain tumors in N-TVA/*Ink4a/Arf null* mice under 100 days of age and deletion of the *Ink4a/Arf* locus alone is insufficient for tumorigenesis within this time period (Serrano *et al.*, 1996; Sharpless *et al.*, 2001).

Gliomas induced by BRAF in the context of Ink4a/Arf-deficiency are distinct from those induced with activated Akt

Tumors arising in mice infected with Akt and KRas^{G12D} or BRAF^{V600E} resembled highly invasive GBM (WHO Grade IV) histologically; both possessed a diffuse growth pattern and contained large confluent geographic necrosis that is well-demarcated from the viable tumor (Figures 2 and 3). In the context of activated Akt, BRAF^{V600E} tumors were extremely pleomorphic, and contained a spectrum of cellular morphology ranging from very small round cells to spindle cells and giant cells (Figure 2). KRas^{G12D} tumors were typically more glial in appearance (Figure 3) and demonstrated extremely pronounced angiogenesis compared to the other tumors in the context of activated Akt (Figure 2). In contrast, KRas^{G12D} tumors arsing in the context of *Ink4a/Arf*-deficiency were much less necrotic than Akt/KRas^{G12D} tumors and possessed a spindle cell tumor morphology with a diffuse and monotonous growth pattern that lacked prominent vascular proliferation. These tumors were relatively well demarcated and not infiltrative, but invasion was seen to progress through the subarachnoid or the Virchow-Robin perivascular space (Figure 2). The phenotype of tumors arising in mice expressing BRAF^{V600E} in the absence of *Ink4a/Arf* was typified by a diffuse monotypic and monomorphic growth pattern with the tumors cells demonstrating angulated pleomorphic nuclei. These tumors did not possess a prominent vasculature and there was no evidence of necrosis. They grew into the subarachnoid space but were well-demarcated and not infiltrative (Figure 2). Despite the significant histological differences between the tumors arising in mice infected with Akt and KRas^{G12D}, Akt and BRAF^{V600E}, or Cre and BRAF^{V600E}, there was no significant difference in tumor incidence, latency, or lethality ($P < 0.1$). In contrast, both tumor lethality and penetrance were significantly higher in mice infected with Cre and KRas^{G12D} with all mice succumbing to disease in less than 60 days (Figure 1c) ($P < 3 \times 10^{-7}$).

Gliomas induced by BRAF in the context of Ink4a/Arf-deficiency are undifferentiated

Expression of BRAF, $KRas^{G12D}$ and Akt in the tumors was confirmed using immunohistochemistry (IHC) for epitope tags V5, FLAG, and HA, respectively. Deletion of the *Ink4a/Arf* locus in tumors induced by Cre infection was established by IHC for $p19^{ARF}$ (Figure 3). IHC also demonstrated that Akt/$KRas^{G12D}$ and Akt/$BRAF^{V600E}$ tumors expressed both the glial differentiation marker GFAP and the oligodendrocyte differentiation marker Olig2, however GFAP expression was absent in tumors lacking *Ink4a/Arf* expression. Interestingly, Olig2 expression was present in Cre/$KRas^{G12D}$ tumors, but absent in Cre/$BRAF^{V600E}$ tumors (Figures 4 and 5). Expression of the stem cell marker nestin was observed in Cre/$BRAF^{V600E}$ and Cre/$KRas^{G12D}$ tumors but was variable and weak in Akt/$BRAF^{V600E}$ and Akt/$KRas^{G12D}$ tumors (Figures 4 and 5). Expression of the glial marker S100 was variable in the majority of tumors but entirely absent in Cre/$BRAF^{V600E}$ tumors (Supplementary Figure 4).

MAPK activation is present in all gliomas induced with either $KRas^{G12D}$ or $BRAF^{V600E}$

MAPK pathway activation within the tumors was confirmed using IHC for phosphorylated Erk (P-Erk; Figure 6a-d). While MAPK activation was observed in all gliomas induced with either $KRas^{G12D}$ or $BRAF^{V600E}$, P-Erk reactivity was considerably higher in gliomas induced with $KRas^{G12D}$ than those induced with $BRAF^{V600E}$. Interestingly, P-Erk reactivity was strongest in tumor cells at the leading edge and low or absent within the center in Cre/$BRAF^{V600E}$ tumors.

Tumor vasculature was assessed by IHC using an antibody to endomucin (Figure 6e-h). The Akt/$KRas^{G12D}$ tumors were highly vascular but the vessels were abnormal (Figure 6e). Assessment of cellular proliferation using IHC for the cellular proliferation marker Ki67 demonstrated that all of the tumors were highly proliferative regardless of context (Figure 6i-l). IHC for the neuronal differentiation marker Synaptophysin was performed to rule out the possibility that the Cre/$BRAF^{V600E}$ tumors were primitive neuroectodermal tumors (Supplementary Figure 5). A summary comparison of glioma morphology and histology is provided in Supplementary Table 1.

Discussion

In the context of activated BRAF, loss of *Ink4a/Arf* appears to be equivalent to gain of Akt in this model. Infection of neural progenitor cells expressing TVA under the control of the nestin promoter in *Ink4a/Arf* $^{lox/lox}$ mice by RCASBP(A)Cre causes a deletion of the *Ink4a/Arf* locus leading to immortalization, loss of cell cycle control, and tumor growth in the presence of activated MAPK (Sharpless *et al.*, 2001; Uhrbom *et al.*, 2002; Uhrbom *et al.*, 2005). Likewise, activation of Akt in these cells also promotes tumor growth in the presence of activated MAPK (Holland *et al.*, 2000; Holmen and Williams, 2005). Akt signaling inhibits apoptosis and promotes proliferation through phosphorylation/inactivation of Bad, forkhead transcription factors, and caspase-9. Akt also regulates the cell cycle by preventing GSK-3β mediated phosphorylation and degradation of oncogenes including β-catenin, cyclin D1, cyclin E, $p21^{CIP1}$, and Myc (Lizcano *et al.*, 2000). Akt activates protein synthesis and inactivation of the eIF4BP1 leading to angiogenesis in both HIF-dependent and independent

pathways via TSC2, mTOR, p70S6 kinase and VEGF (Mizoguchi *et al.*, 2004; Riemenschneider *et al.*, 2006).

Tumors induced by BRAF^{V600E} in the context of *Ink4a/Arf*-deficiency lack the hallmarks of diffuse infiltration, necrosis and aberrant vascularization normally ascribed to aggressive gliomas. They do not express the glial differentiation markers GFAP or S100, or the oligodendrocyte differentiation marker Olig2 (Dai *et al.*, 2005), but strongly express the stem cell marker nestin suggesting that they have remained in an undifferentiated state. In contrast, BRAF^{V600E} tumors in the context of activated Akt more closely resemble GBM and are more similar to Akt/KRas^{G12D} tumors albeit with less vascularity. Akt pathway activation also promotes astrocytic differentiation further explaining the differences in morphology between Akt and Cre induced *Ink4a/Arf*-null tumors (Dai and Holland, 2003; Hu *et al.*, 2005). Although Cre/KRas^{G12D} tumors were distinct from Cre/BRAF^{V600E} tumors, they were more similar to Akt/BRAF^{V600E} than Akt/KRas^{G12D} tumors in terms of the level of invasion and necrosis observed. Both the BRAF^{V600E} and KRas^{G12D} *Ink4a/Arf*-null tumors were considerably more proliferative than the Akt tumors. This is not surprising as they have lost control over both cell cycle progression and arrest as a result of p53 and pRb pathway inactivation. Furthermore, the presence of angulated pleomorphic nuclei and strong nestin immunoreactivity suggests that these tumors are not benign low grade lesions, but aggressive gliomas. High nestin expression is typically found in malignant high grade primary brain tumors, whereas lower grade gliomas express low levels of nestin (Dahlstrand *et al.*, 1992). It is possible that infection of nestin expressing neural progenitor cells with viruses containing BRAF^{V600E} and activated Akt induces astrocytic differentiation. In view of the fact that human gliomas differ markedly in grade and histological appearance it is not surprising that gliomas induced with different oncogenes give rise to tumors with distinct histology. Although BRAF^{V600E} and KRas^{G12D} both promote glioma formation through MAPK activation, KRas activates additional downstream effectors also known to be dysregulated in GBM (e.g., PI3K and RAL). These differences in regulation and downstream effectors may explain the different morphology seen between the BRAF^{V600E} and KRas^{G12D} induced gliomas particularly as several RAS effectors have roles in hypoxia and vascular growth.

It is interesting to note that tumors induced by BRAF^{V600E} in the context of *Ink4a/Arf*-deficiency are quite different from tumors induced by active CRAF in the context of *Arf* loss (Lyustikman *et al.*, 2008). The CRAF *Arf*-null tumors presented with histological features similar to GBM, which are absent in BRAF^{V600E} *Ink4a/Arf*-null tumors. The CRAF tumors are described as having a ‘spindle-cell sarcoma-like morphology’ containing pronounced angiogenesis, giant cells, and ‘pseudopalisading necrosis’ common to GBM. KRas^{G12D} *Arf*-null tumors displayed the same phenotype and both tumor types expressed GFAP and Nestin (Lyustikman *et al.*, 2008). Since the phenotype of the KRas^{G12D} *Arf*-null tumors is similar to what we observed with KRas^{G12D} in the absence of both *Ink4a* and *Arf*, the additional loss of *Ink4a* in our experiments is unlikely to be the cause of the phenotypic differences between BRAF^{V600E} and activated CRAF. Genetic studies in mice have revealed that the RAF proteins have non-redundant functions in development, which suggests that the different isoforms perform distinct functions (Pritchard *et al.*, 1996; Wojnowski *et al.*, 1998;

Wojnowski *et al.*, 1997). In addition, there are known differences in how the RAF proteins are regulated. Phosphorylation of S338 and Y341 by Src in the N-region is required for activation of CRAF by Ras (Chong *et al.*, 2001). These sites are not conserved in BRAF, which is constitutively phosphorylated allowing activation by Ras alone (Wellbrock *et al.*, 2004). BRAF contains three negative regulatory Akt phosphorylation sites (Ser365, Ser429 and Thr440), Akt signaling reduces BRAF activity and inhibition of Akt with the PI3K inhibitor LY294002 leads to increased BRAF activity (Guan *et al.*, 2000). These sites are absent in CRAF (Guan *et al.*, 2000) and the *CRAF* mutant studied, 22W (Stanton *et al.*, 1989), lacks the N-terminal 305 amino acids, which contain the CR1 and CR2 regulatory domains (Wellbrock *et al.*, 2004). Therefore, it is highly likely that there are significant differences in the signaling activity of the mutants studied.

Primary glioblastoma, Giant cell glioblastoma and gliosarcoma, a glioblastoma subtype with focal aberrant mesenchymal differentiation, differ in both their histological appearance and mutation spectrum (Jones *et al.*, 1991; Paulus and Jellinger, 1992; Reis *et al.*, 2000). Our results suggest that a high degree of Akt activation may be necessary for Giant cell formation since this phenotype was only observed in the presence of activated Akt and these cells demonstrated strong Akt immunoreactivity. In contrast, the cells of KRas^{G12D} *Ink4a/Arf*-null tumors were spindle cell like in appearance and did not demonstrate GFAP reactivity, which is frequently seen in areas of gliosarcomas and spindle cell gliomas (Uhrbom *et al.*, 2002). Tumor vasculature was more prominent in KRas^{G12D} and Akt induced tumors than KRas^{G12D} *Ink4a/Arf*-null tumors; however, this vasculature was highly abnormal and not necessary for tumor development since the *Ink4a/Arf*-null tumors contained a well ordered vasculature with much less necrosis than the Akt tumors.

Despite the common occurrence of BRAF mutations in PAs, none of the BRAF^{V600E} tumors resembled PA in appearance or grade. The BRAF-*KIAA1549* fusion gene found in the majority of PAs shows a deletion of either two or all three of the negative regulatory AKT consensus phosphorylation sites, which results in elevated BRAF kinase activity (Jones *et al.*, 2008) and this may be partly responsible for the morphological differences. Moreover, mutations that target the p53 pathway are seen in low-grade astrocytomas and loss of p53 function can act as an initiating event in astrocytoma pathogenesis (Marino *et al.*, 2000; Ohgaki and Kleihues, 2007). pRb pathway inactivation and Akt activation are typically only seen in high-grade glioma (Hamel *et al.*, 1993; Ohgaki and Kleihues, 2007) and loss of pRb function is considered to be involved in the progression from benign to highly malignant astrocytomas (Kleihues *et al.*, 1993). It is likely that BRAF^{V600E} activation of the MAPK pathway in combination with *Ink4a/Arf* loss prevents or provides no signal for differentiation leaving the cells in an immature state.

Cancers with BRAF mutations often evolve to become addicted to this signaling pathway. Given that inhibition of RAF or MEK in melanoma cells lines with BRAF mutations causes the cells to undergo G1 arrest and leads to apoptosis via Bim and Bmf activation (VanBrocklin *et al.*, 2009), combination therapy with RAF or MEK inhibitors and a BH3 mimetic (e.g., ABT-737) may prove beneficial. On the other hand, MEK/ERK signaling represents only one arm of the tumor growth and survival network in gliomas with Ras or RTK mutations, and in many cases the ERK and PI3K pathways regulate a common set of

downstream apoptotic regulators (e.g., Bad, Mcl-1, Bcl-x_L and Bcl2) (Balmanno and Cook, 2009). In these cases, the combination of a BH3 mimetic with MEK/RAF and PI3K inhibitors may prove necessary.

In conclusion, $BRAF^{V600E}$ can substitute for Ras mutations in the development of GBM when combined with Akt. In contrast, $BRAF^{V600E}$ tumors induced in the context of *Ink4a/Arf*$^{-}$ deficiency do not resemble GBM, but are highly malignant. Due to the high expression of RAF proteins in high grade glioma, the incidence of BRAF mutations in low grade gliomas, and the reliance of these tumors on active ERK/MAPK signaling for survival (Holmen and Williams, 2005), inhibition of RAF or MEK may represent an appropriate therapeutic strategy for gliomas with altered BRAF activity.

Materials and Methods

Transgenic mice

Nestin-TVA (N-TVA) mice have been described (Holland *et al.*, 1998a) and were purchased from the Van Andel Research Institute mouse repository. *Ink4a/Arf* $^{lox/lox}$ mice have also been described and were a kind gift from Ronald DePinho (Aguirre *et al.*, 2003). All experiments were performed in compliance with the “Care and Use of Animals” and were approved by the IACUC prior to experimentation.

Vector constructs

The retroviral vectors used in this study were replication-competent avian leukosis virus long terminal repeat, splice acceptor, Bryan polymerase-containing vectors of envelope subgroup A (Holmen *et al.*, 1999). RCASBP(A)$KRas^{G12D}$ and RCASBP(A)*Akt* have been previously described (Holland *et al.*, 2000; Holmen and Williams, 2005). The N-terminus of KRas has a FLAG epitope tag and Akt contains an HA epitope tag at the C-terminus. The Akt used is the activated form designated Akt-Myr Δ11-60 (Holland *et al.*, 2000). RCASBP(A)*Cre* was a gift from Eric Holland (MSKCC) and the pCDNA3.1 constructs containing human wild-type (NM_04333.4) and $BRAF^{V600}$ were gifts from Martin McMahon (UCSF). To generate pENTR3C-*BRAF-wt* and $BRAF^{V600E}$, the pCDNA3.1-*BRAF* constructs were digested with *Pme* I and the 2.4 Kb *BRAF* fragments were cloned into pENTR3C (Invitrogen, Carlsbad, CA) digested with *Dra* I and *Eco R*V. A V5 epitope tag was inserted at the C-terminus of $BRAF^{V600E}$ by cloning the 1.8 Kb *Kpn* I and *Xba* I fragment into pCDNA6/V5HisA (Invitrogen) cut with the same enzymes. The fragment along with the V5 sequence was excised as a *Kpn* I-*Pme* I fragment and inserted back into pENTR3C-$BRAF^{V600E}$ digested with *Xba* I, filled in with Klenow, and digested with *Kpn* I. RCASBP(A)$BRAF^{V600E}$-*V5* was generated by mixing pENTR3C-$BRAF^{V600E}$-*V5* with the RCASBP(A) destination vector in the presence of the LR Clonase Enzyme Mix as described (Bromberg-White *et al.*, 2004).

Cell culture

DF-1 cells were grown in DMEM-high glucose supplemented with 10% FBS (Hyclone, Logan, UT), 1 × penicillin/streptomycin, and maintained at 39 °C (Schaefer-Klein *et al.*, 1998). Primary astrocytes were isolated from the brains of Nestin-TVA-positive newborn

mice. Single cells were obtained by mincing the tissue followed by digestion in 0.05% trypsin (Invitrogen) for 30 min at 37 °C. The cells were resuspended in RPMI 1640 (Invitrogen) with 5% FBS and 1 × penicillin/streptomycin (Invitrogen).

Growth in Soft Agar

To assess anchorage-independent growth, 1.5×10^5 cells were suspended in 0.35% Difco agar noble (Becton Dickinson, Sparks, MD) in RPMI with 10% FBS and layered over pre-solidified 0.65% Difco Noble Agar in RPMI with 10% FBS per well of a 6-well dish. Each cell line was assayed in triplicate.

Virus propagation

Virus infection was initiated by calcium phosphate transfection of plasmid DNA that contained the proviral retroviral vector. In standard transfections, DF-1 cells were plated at 30% confluency, allowed to attach (2–3 h), and 10 μg of purified plasmid DNA was introduced by the calcium phosphate precipitation method as previously described (Holmen *et al.*, 1999). Viral spread was monitored by assaying culture supernatants for ALV capsid protein by ELISA as previously described (Smith *et al.*, 1979).

Viral infections in vitro

Astrocytes were seeded in 6-well plates at a density of 5×10^4 cells/well and were maintained in RPMI 1640 with 5% FBS, 1 × penicillin/streptomycin at 37 °C. After the cells attached, the medium was removed and replaced with 1 ml of filtered virus-containing medium in the presence of 8 μg/ml polybrene (Sigma, St. Louis, MO) for 2 h at 37 °C. The virus was removed and replaced with fresh medium, and the cells were incubated at 37 °C for 1 h. Cells were infected again for another 2 h, after which the virus-containing medium was replaced with fresh medium and the cells were incubated overnight at 37 °C.

Viral infections in vivo

The N-TVA line was crossed to *Ink4a/Arf* $^{lox/lox}$ mice, to generate N-TVA/*Ink4a/Arf* $^{lox/+}$ mice. These mice were then intercrossed to generate N-TVA/*Ink4a/Arf* $^{lox/lox}$ mice. The *lox* sites flank exons 2 and 3 of this locus such that Cre-mediated excision eliminates both $p16^{INK4A}$ and $p19^{ARF}$. Infected DF-1 cells from a confluent culture in a 10-cm dish were trypsinized, pelleted, resuspended in 50 μl PBS, and placed on ice. Newborn N-TVA/*Ink4a/Arf* $^{lox/lox}$ mice were injected intracranially 2 mm ventral from bregma (intersection of the coronal and sagittal sutures) with 5μl of infected DF-1 cells using a gas-tight Hamilton syringe. Cohorts were injected with RCASBP(A)$BRAF^{V600E}$ or RCASBP(A)$KRas^{G12D}$ alone or in combination with RCASBP(A)*Cre* or RCASBP(A)*Akt*. Censored survival data was analyzed using a log-rank test of the Kaplan-Meier estimate of survival.

Western blotting

Western blots were immunostained for Akt-HA using an anti-HA monoclonal antibody (HA.11, Covance, Berkely, CA) at a 1:1000 dilution; $BRAF^{V600E}$-V5 using a mouse monoclonal antibody targeting V5 (R960-25, Invitrogen) at a 1:1000 dilution; $KRas^{G12D}$ using a pan-RAS antibody (05-516, Millipore, Temeculah, CA) diluted 1:1000, and anti-α-

tubulin (T9026, Sigma) at a 1:5000 dilution. Detection of MAPK activation was performed using a 1:1000 dilution of a rabbit monoclonal antibody directed against phosphorylation of Erk at Thr202 and Tyr 204 (4370,Cell Signaling, Boston, MA). Detection of total Erk protein levels was performed using a 1:5000 dilution of anti-Erk antibody (9102, Cell Signaling). Detection of BRAF was performed using a 1:1000 dilution of anti-BRAF antibody (9434, Cell Signaling). The blots were then incubated with an anti-mouse or rabbit IgG-HRP secondary antibody diluted 1:2000 (Cell Signaling) for 1 h at room temperature. The blots were incubated with ECL (Amersham, Piscataway, NJ), and exposed to film.

Immunohistochemistry

Tissues were paraffin embedded and 5-μm sections were adhered to glass slides. Sections were stained with H&E or left unstained for IHC. Antigen retrieval was performed in 'Diva Decloaking' buffer (Biocare medical, Concord, CA) by boiling for 10 min. Sections were treated with 3% hydrogen peroxide and blocked in Background Sniper (Biocare medical) for 10 min. Primary antibodies were diluted in Renaissance background reducing diluent (Biocare medical). Sections were incubated overnight at 4C and probed with Mach 4 rabbit polymer reagent (Biocare medical) or Mach 4 mouse probe for 15 min followed by Mach 4 polymer for 15 min for mouse monoclonal antibodies. Visualization was carried out with DAB (Biocare medical). Akt expression was detected using an antibody to the HA epitope (HA.11, Covance) (diluted 1:1000). BRAF expression was detected using an antibody to the V5 epitope (Invitrogen) (diluted 1:200), Cell proliferation was detected using an antibody to Ki67 (M7246, Dako, Carpinteria, CA) (diluted 1:50). The following additional antibodies were used at a 1:200 dilution: GFAP (ab7260, Abcam, Cambridge, MA), Olig2 (ab33427, Abcam), Nestin (ab6142, Abcam), $p19^{ARF}$ (ab80, Abcam), Synaptophysin (ab32127, Abcam), S100 (Z0311, Dako), and Endomucin (sc65495, Santa Cruz Biotechnology, Santa Cruz, CA). Ras expression was detected using an antibody to the FLAG epitope (M2, Sigma). Detection of MAPK activation was performed using a 1:100 dilution of a phospho-Erk antibody (4370, Cell Signaling).

Supplementary Material

Refer to Web version on PubMed Central for supplementary material.

Acknowledgments

This work was supported by the Nevada Cancer Institute, the National Brain Tumor Foundation, and RSG-06-198-01-TBE from the American Cancer Society. We thank Nick Henderson and Robert Kirsh for animal husbandry. We also thank Eric Holland, Martin McMahon, and Ronald DePinho for reagents. S.L.H. designed the research; J.P.R., M.W.V. and S.L.H. performed the research; S.B. performed the pathological analysis; D.L.S and A.R.G. provided technical support; J.P.R. and S.L.H. prepared the images and wrote the paper.

Bibliography

Aguirre AJ, Bardeesy N, Sinha M, Lopez L, Tuveson DA, Horner J, et al. Activated Kras and Ink4a/Arf deficiency cooperate to produce metastatic pancreatic ductal adenocarcinoma. Genes Dev. 2003; 17:3112–26. [PubMed: 14681207]

Balmanno K, Cook SJ. Tumour cell survival signalling by the ERK1/2 pathway. Cell Death Differ. 2009; 16:368–77. [PubMed: 18846109]

Barnier JV, Papin C, Eychene A, Lecoq O, Calothy G. The mouse B-raf gene encodes multiple protein isoforms with tissue-specific expression. J Biol Chem. 1995; 270:23381–9. [PubMed: 7559496]

Basto D, Trovisco V, Lopes JM, Martins A, Pardal F, Soares P, et al. Mutation analysis of B-RAF gene in human gliomas. Acta Neuropathol. 2005; 109:207–10. [PubMed: 15791479]

Bromberg-White JL, Webb CP, Patacsil VS, Miranti CK, Williams BO, Holmen SL. Delivery of short hairpin RNA sequences by using a replication-competent avian retroviral vector. J Virol. 2004; 78:4914–6. [PubMed: 15078973]

Chin L, Pomerantz J, DePinho RA. The INK4a/ARF tumor suppressor: one gene--two products--two pathways. Trends Biochem Sci. 1998; 23:291–6. [PubMed: 9757829]

Chong H, Lee J, Guan KL. Positive and negative regulation of Raf kinase activity and function by phosphorylation. EMBO J. 2001; 20:3716–27. [PubMed: 11447113]

Dahlstrand J, Collins VP, Lendahl U. Expression of the class VI intermediate filament nestin in human central nervous system tumors. Cancer Res. 1992; 52:5334–41. [PubMed: 1382841]

Dai C, Holland EC. Astrocyte differentiation states and glioma formation. Cancer J. 2003; 9:72–81. [PubMed: 12784872]

Dai C, Lyustikman Y, Shih A, Hu X, Fuller GN, Rosenblum M, et al. The characteristics of astrocytomas and oligodendrogliomas are caused by two distinct and interchangeable signaling formats. Neoplasia. 2005; 7:397–406. [PubMed: 15967117]

Davies H, Bignell GR, Cox C, Stephens P, Edkins S, Clegg S, et al. Mutations of the BRAF gene in human cancer. Nature. 2002; 417:949–54. [PubMed: 12068308]

Furnari FB, Fenton T, Bachoo RM, Mukasa A, Stommel JM, Stegh A, et al. Malignant astrocytic glioma: genetics, biology, and paths to treatment. Genes Dev. 2007; 21:2683–710. [PubMed: 17974913]

Guan KL, Figueroa C, Brtva TR, Zhu T, Taylor J, Barber TD, et al. Negative regulation of the serine/threonine kinase B-Raf by Akt. J Biol Chem. 2000; 275:27354–9. [PubMed: 10869359]

Hamel W, Westphal M, Shepard HM. Loss in expression of the retinoblastoma gene product in human gliomas is associated with advanced disease. J Neurooncol. 1993; 16:159–65. [PubMed: 8289093]

Hill JR, Kuriyama N, Kuriyama H, Israel MA. Molecular genetics of brain tumors. Arch Neurol. 1999; 56:439–41. [PubMed: 10199332]

Holland EC, Celestino J, Dai C, Schaefer L, Sawaya RE, Fuller GN. Combined activation of Ras and Akt in neural progenitors induces glioblastoma formation in mice. Nat Genet. 2000; 25:55–7. [PubMed: 10802656]

Holland EC, Hively WP, DePinho RA, Varmus HE. A constitutively active epidermal growth factor receptor cooperates with disruption of G1 cell-cycle arrest pathways to induce glioma-like lesions in mice. Genes Dev. 1998a; 12:3675–85. [PubMed: 9851974]

Holland EC, Hively WP, Gallo V, Varmus HE. Modeling mutations in the G1 arrest pathway in human gliomas: overexpression of CDK4 but not loss of INK4a-ARF induces hyperploidy in cultured mouse astrocytes. Genes Dev. 1998b; 12:3644–9. [PubMed: 9851971]

Holmen SL, Salter DW, Payne WS, Dodgson JB, Hughes SH, Federspiel MJ. Soluble forms of the subgroup A avian leukosis virus [ALV(A)] receptor Tva significantly inhibit ALV(A) infection in vitro and in vivo. J Virol. 1999; 73:10051–60. [PubMed: 10559319]

Holmen SL, Williams BO. Essential role for Ras signaling in glioblastoma maintenance. Cancer Res. 2005; 65:8250–5. [PubMed: 16166301]

Hu X, Pandolfi PP, Li Y, Koutcher JA, Rosenblum M, Holland EC. mTOR promotes survival and astrocytic characteristics induced by Pten/AKT signaling in glioblastoma. Neoplasia. 2005; 7:356–68. [PubMed: 15967113]

Jeuken J, van den Broecke C, Gijsen S, Boots-Sprenger S, Wesseling P. RAS/RAF pathway activation in gliomas: the result of copy number gains rather than activating mutations. Acta Neuropathol. 2007; 114:121–33. [PubMed: 17588166]

Jones DT, Kocialkowski S, Liu L, Pearson DM, Backlund LM, Ichimura K, et al. Tandem duplication producing a novel oncogenic BRAF fusion gene defines the majority of pilocytic astrocytomas. Cancer Res. 2008; 68:8673–7. [PubMed: 18974108]

Jones DT, Kocialkowski S, Liu L, Pearson DM, Ichimura K, Collins VP. Oncogenic RAF1 rearrangement and a novel BRAF mutation as alternatives to KIAA1549:BRAF fusion in

activating the MAPK pathway in pilocytic astrocytoma. Oncogene. 2009; 28:2119–23. [PubMed: 19363522]

Jones H, Steart PV, Weller RO. Spindle-cell glioblastoma or gliosarcoma? Neuropathol Appl Neurobiol. 1991; 17:177–87. [PubMed: 1653908]

Kleihues P, Burger PC, Scheithauer BW. The new WHO classification of brain tumours. Brain Pathol. 1993; 3:255–68. [PubMed: 8293185]

Lizcano JM, Morrice N, Cohen P. Regulation of BAD by cAMP-dependent protein kinase is mediated via phosphorylation of a novel site, Ser155. Biochem J. 2000; 349:547–57. [PubMed: 10880354]

Louis DN, Ohgaki H, Wiestler OD, Cavenee WK, Burger PC, Jouvet A, et al. The 2007 WHO classification of tumours of the central nervous system. Acta Neuropathol. 2007; 114:97–109. [PubMed: 17618441]

Lyustikman Y, Momota H, Pao W, Holland EC. Constitutive activation of Raf-1 induces glioma formation in mice. Neoplasia. 2008; 10:501–10. [PubMed: 18472967]

Marino S, Vooijs M, van Der Gulden H, Jonkers J, Berns A. Induction of medulloblastomas in p53-null mutant mice by somatic inactivation of Rb in the external granular layer cells of the cerebellum. Genes Dev. 2000; 14:994–1004. [PubMed: 10783170]

Mizoguchi M, Nutt CL, Mohapatra G, Louis DN. Genetic alterations of phosphoinositide 3- kinase subunit genes in human glioblastomas. Brain Pathol. 2004; 14:372–7. [PubMed: 15605984]

Ohgaki H, Kleihues P. Genetic pathways to primary and secondary glioblastoma. Am J Pathol. 2007; 170:1445–53. [PubMed: 17456751]

Paulus W, Jellinger K. Desmoplastic spindle-cell glioblastoma or gliosarcoma? Neuropathol Appl Neurobiol. 1992; 18:207–8. [PubMed: 1620280]

Pfister S, Janzarik WG, Remke M, Ernst A, Werft W, Becker N, et al. BRAF gene duplication constitutes a mechanism of MAPK pathway activation in low-grade astrocytomas. J Clin Invest. 2008; 118:1739–49. [PubMed: 18398503]

Pritchard CA, Bolin L, Slattery R, Murray R, McMahon M. Post-natal lethality and neurological and gastrointestinal defects in mice with targeted disruption of the A-Raf protein kinase gene. Curr Biol. 1996; 6:614–7. [PubMed: 8805280]

Quelle DE, Zindy F, Ashmun RA, Sherr CJ. Alternative reading frames of the INK4a tumor suppressor gene encode two unrelated proteins capable of inducing cell cycle arrest. Cell. 1995; 83:993–1000. [PubMed: 8521522]

Reis RM, Konu-Leblebicioglu D, Lopes JM, Kleihues P, Ohgaki H. Genetic profile of gliosarcomas. Am J Pathol. 2000; 156:425–32. [PubMed: 10666371]

Riemenschneider MJ, Betensky RA, Pasedag SM, Louis DN. AKT activation in human glioblastomas enhances proliferation via TSC2 and S6 kinase signaling. Cancer Res. 2006; 66:5618–23. [PubMed: 16740698]

Roussel MF. The INK4 family of cell cycle inhibitors in cancer. Oncogene. 1999; 18:5311–7. [PubMed: 10498883]

Schaefer-Klein J, Givol I, Barsov EV, Whitcomb JM, VanBrocklin M, Foster DN, et al. The EV-O-derived cell line DF-1 supports the efficient replication of avian leukosis-sarcoma viruses and vectors. Virology. 1998; 248:305–11. [PubMed: 9721239]

Serrano M, Lee H, Chin L, Cordon-Cardo C, Beach D, DePinho RA. Role of the INK4a locus in tumor suppression and cell mortality. Cell. 1996; 85:27–37. [PubMed: 8620534]

Sharpless NE, Bardeesy N, Lee KH, Carrasco D, Castrillon DH, Aguirre AJ, et al. Loss of p16Ink4a with retention of p19Arf predisposes mice to tumorigenesis. Nature. 2001; 413:86–91. [PubMed: 11544531]

Smith EJ, Fadly A, Okazaki W. An enzyme-linked immunosorbent assay for detecting avian leukosis-sarcoma viruses. Avian Dis. 1979; 23:698–707. [PubMed: 230808]

Stanton VP Jr. Nichols DW, Laudano AP, Cooper GM. Definition of the human raf amino- terminal regulatory region by deletion mutagenesis. Mol Cell Biol. 1989; 9:639–47. [PubMed: 2710120]

Uhrbom L, Dai C, Celestino JC, Rosenblum MK, Fuller GN, Holland EC. Ink4a-Arf loss cooperates with KRas activation in astrocytes and neural progenitors to generate glioblastomas of various morphologies depending on activated Akt. Cancer Res. 2002; 62:5551–8. [PubMed: 12359767]

Uhrbom L, Kastemar M, Johansson FK, Westermark B, Holland EC. Cell type-specific tumor suppression by Ink4a and Arf in Kras-induced mouse gliomagenesis. Cancer Res. 2005; 65:2065–9. [PubMed: 15781613]

VanBrocklin MW, Verhaegen M, Soengas MS, Holmen SL. Mitogen-activated protein kinase inhibition induces translocation of Bmf to promote apoptosis in melanoma. Cancer Res. 2009; 69:1985–94. [PubMed: 19244105]

Wellbrock C, Karasarides M, Marais R. The RAF proteins take centre stage. Nat Rev Mol Cell Biol. 2004; 5:875–85. [PubMed: 15520807]

Wojnowski L, Stancato LF, Zimmer AM, Hahn H, Beck TW, Larner AC, et al. Craf-1 protein kinase is essential for mouse development. Mech Dev. 1998; 76:141–9. [PubMed: 9767153]

Wojnowski L, Zimmer AM, Beck TW, Hahn H, Bernal R, Rapp UR, et al. Endothelial apoptosis in Braf-deficient mice. Nat Genet. 1997; 16:293–7. [PubMed: 9207797]

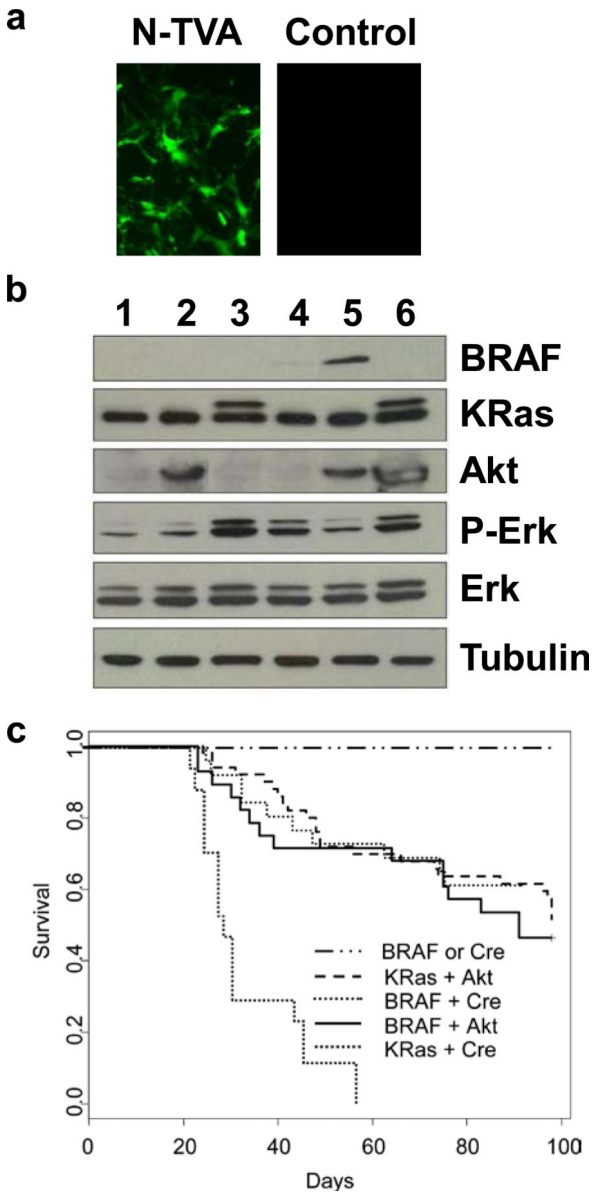

Figure 1. KRas^{G12D} and BRAF^{V600E} cooperate with activated Akt or *Ink4a/Arf* loss to induce gliomas in N-TVA mice

(a) *In vitro* expression of GFP in N-TVA astrocytes. RCASBP(A)GFP infection of N-TVA positive and negative (control) cells in culture confirmed stable and targeted gene delivery of GFP into N-TVA expressing cells. **(b) Western blot analysis of gene expression.** N-TVA-positive immortalized astrocytes were infected in culture with RCASBP(A)*GFP* (lane 1), RCASBP(A)*Akt* (lane 2), RCASBP(A)*KRas*^{G12D} (lane 3), RCASBP(A)*BRAF*^{V600E} (lane 4), RCASBP(A)*BRAF*^{V600E} and RCASBP(A)*Akt* (lane 5), or RCASBP(A)*Akt* and RCASBP(A)*KRas*^{G12D} (lane 6). Lysates were separated on a 4-20% Tris-glycine polyacrylamide gel, transferred to nitrocellulose, and probed with antibodies directed against V5 (BRAF), HA (Akt), pan-RAS (KRas), phoshporylated Erk (P-Erk), or total Erk (Erk) as indicated. The membrane was re-probed with an antibody against α-tubulin (bottom) to ensure equal loading. The Ras blot shows endogenous Ras (lower band) and the virally

delivered KRas (upper band). The virally delivered KRas is a higher molecular weight as a result of the FLAG epitope tag. **(c) Kaplan-Meier percent survival curve.** N-TVA;*Ink4a/Arf*$^{lox/lox}$ mice were injected with the indicated viruses at birth. Censored survival data was analyzed using a log-rank test of the Kaplan-Meier estimate of survival. No tumors were observed in mice injected with BRAF^{V600E} or Cre alone $n = 36$ (solid black line) and it has previously been shown that no tumors form in mice injected with either KRas^{G12D} or Akt alone (Holland *et al.*, 2000). There was no significant difference in survival between KRas^{G12D} + Akt $n = 50$ (red line) BRAF^{V600E} + Cre $n = 26$ (blue line) or BRAF^{V600E} + Akt $n = 28$ (green line). A significant difference in survival was observed between KRas^{G12D} + Cre $n = 17$ (dashed black line) and all of the other conditions, $P < 3 \times 10^{-7}$.

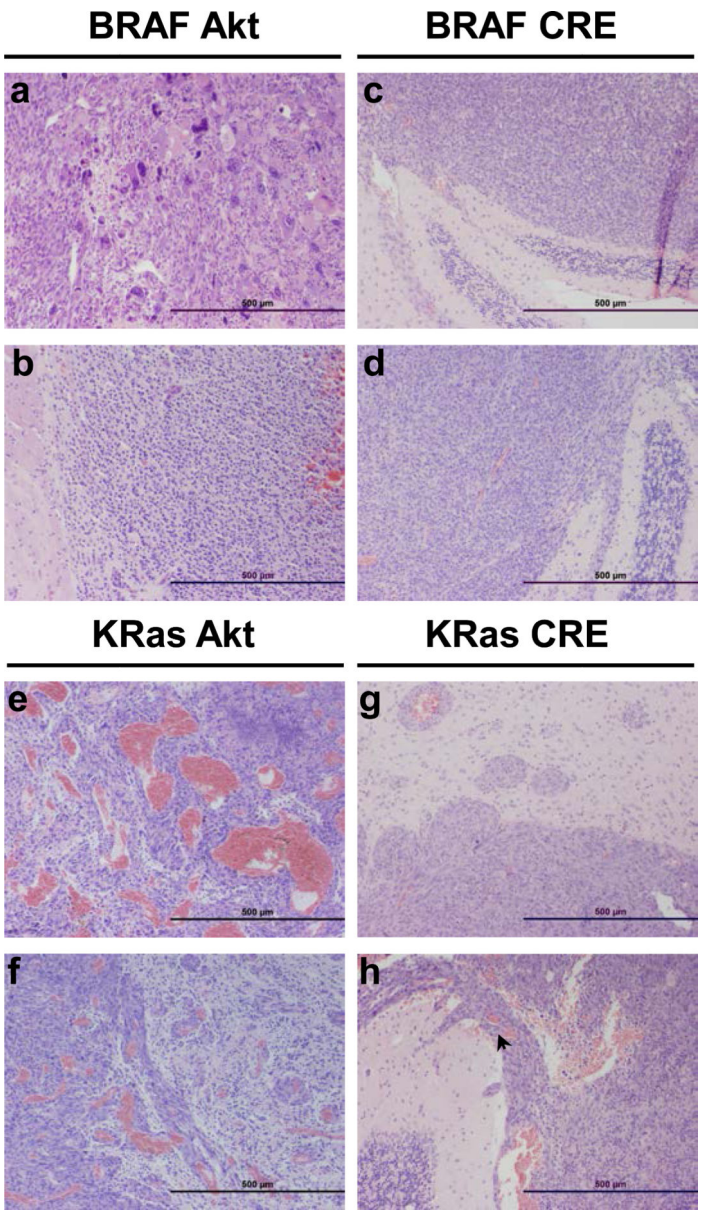

Figure 2. Representative tumors induced by KRas^{G12D} or BRAF^{V600E} in cooperation with activated Akt or Cre *(Ink4a/Arf* loss)

Histological comparison of gliomas induced in N-TVA;*Ink4a/Arf*$^{lox/lox}$ mice after injection with **(a-b)** BRAF^{V600E} + Akt, **(c-d)** BRAF^{V600E} + Cre, **(e-f)** KRas^{G12D} + Akt and **(g-h)** KRas^{G12D} + Cre. Although the CNS border was well defined (**g-h**) and the tumors were not infiltrative, invasion was seen to progress through the subarachnoid space and Virchow-Robin perivascular spaces (arrow, **h**). Scale bars represent 500 μm.

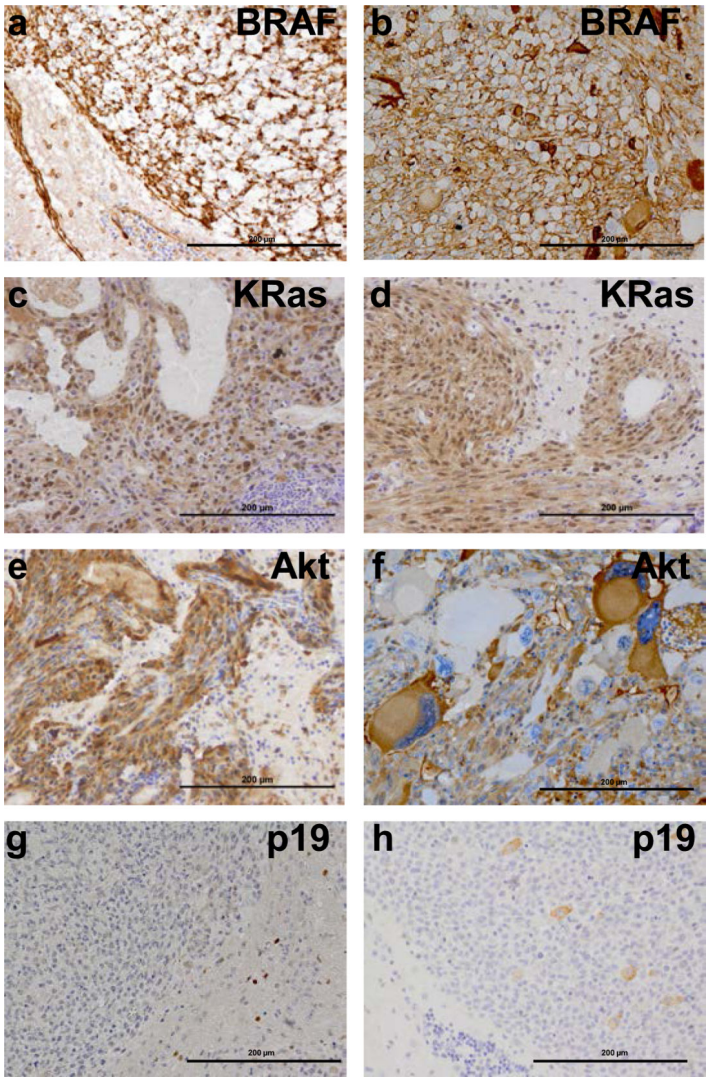

Figure 3. Immunohistochemical confirmation of gene expression in gliomas arising in N-TVA;*Ink4a/Arf*$^{lox/lox}$ mice

(a) IHC for the V5 epitope tag on BRAF^{V600E} in gliomas induced by BRAF^{V600E} + Cre. **(b)** IHC for the V5 epitope tag on BRAF^{V600E} in gliomas induced by BRAF^{V600E} + Akt. **(c)** IHC for the FLAG epitope tag on KRas in gliomas induced by KRas^{G12D} +Akt. **(d)** IHC for the FLAG epitope tag on KRas^{G12D} in gliomas induced by KRas^{G12D} + Cre. **(e)** IHC for the HA epitope tag on Akt in gliomas induced by KRas^{G12D} + Akt. **(f)** IHC for the HA epitope tag on Akt in gliomas induced by BRAF^{V600E} + AKT. IHC for p19 indicates loss of p19 expression in **(g)** KRas^{G12D}, **(f)** BRAF^{V600E} + Cre induced gliomas. Scale bars represent 200 μm.

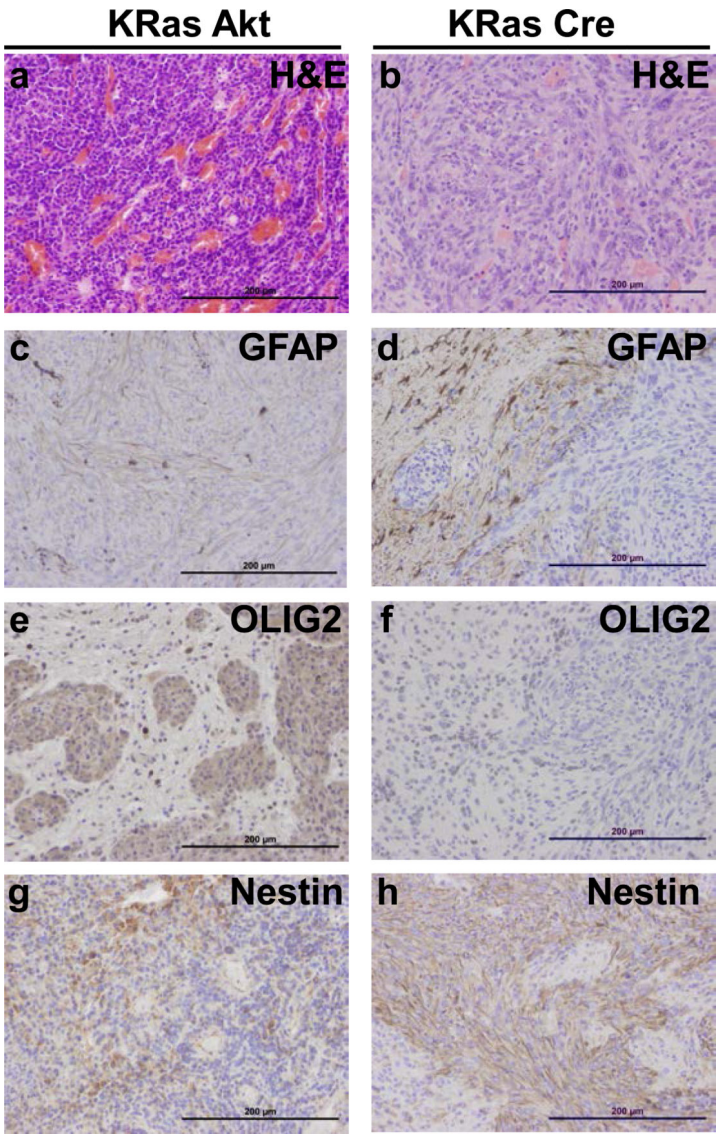

Figure 4. Expression of astrocyte and oligodendrocyte markers in gliomas induced with $KRas^{G12D}$

(a-b) Corresponding H&E sections for histological comparison with IHC analysis. **(c-d)** Expression of the astrocyte marker GFAP. **(e-f)** Expression of the oligodendrocyte marker Olig2. **(g-h)** Expression of the neural progenitor cell marker Nestin. Scale bars represent 200 μm.

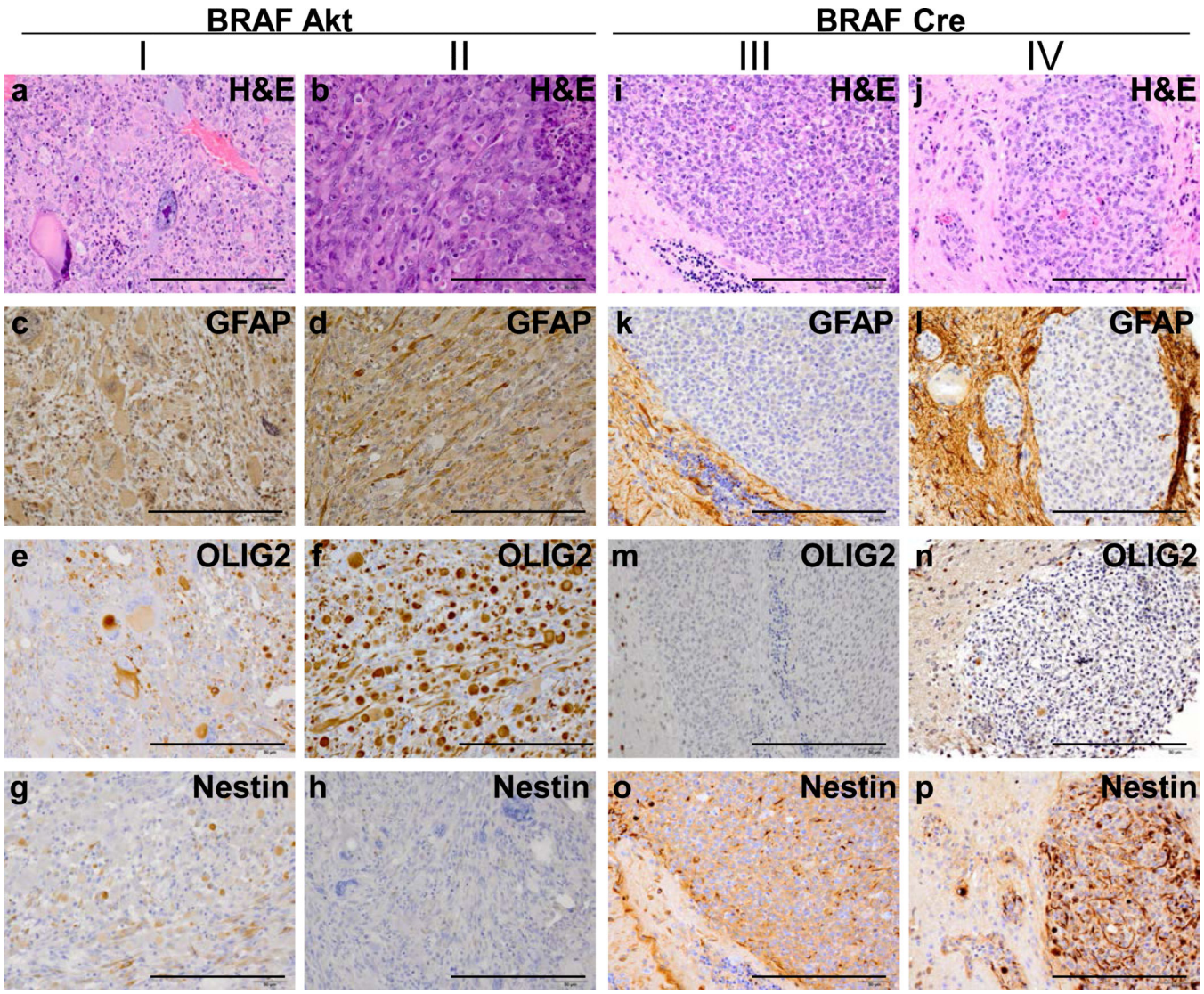

Figure 5. Expression of astrocyte and oligodendrocyte markers in gliomas induced with BRAF^{V600E}

(I-II) BRAF^{V600E} gliomas induced with activated Akt were highly pleomorphic in expression and appearance so two examples are highlighted for comparison with **(III-IV)** the highly monomorphic nature of BRAF^{V600E} gliomas in the context of *Ink4a/Arf* loss. **(a-b and i-j)** Corresponding H&E sections for histological comparison with IHC analysis. **(c-f and k-l)** Expression of the astrocyte marker GFAP. **(e-f and m-n)** Expression of the oligodendrocyte marker Olig2. **(g-h and o-p)** Expression of the neural progenitor cell marker Nestin. Scale bars represent 200 μm.

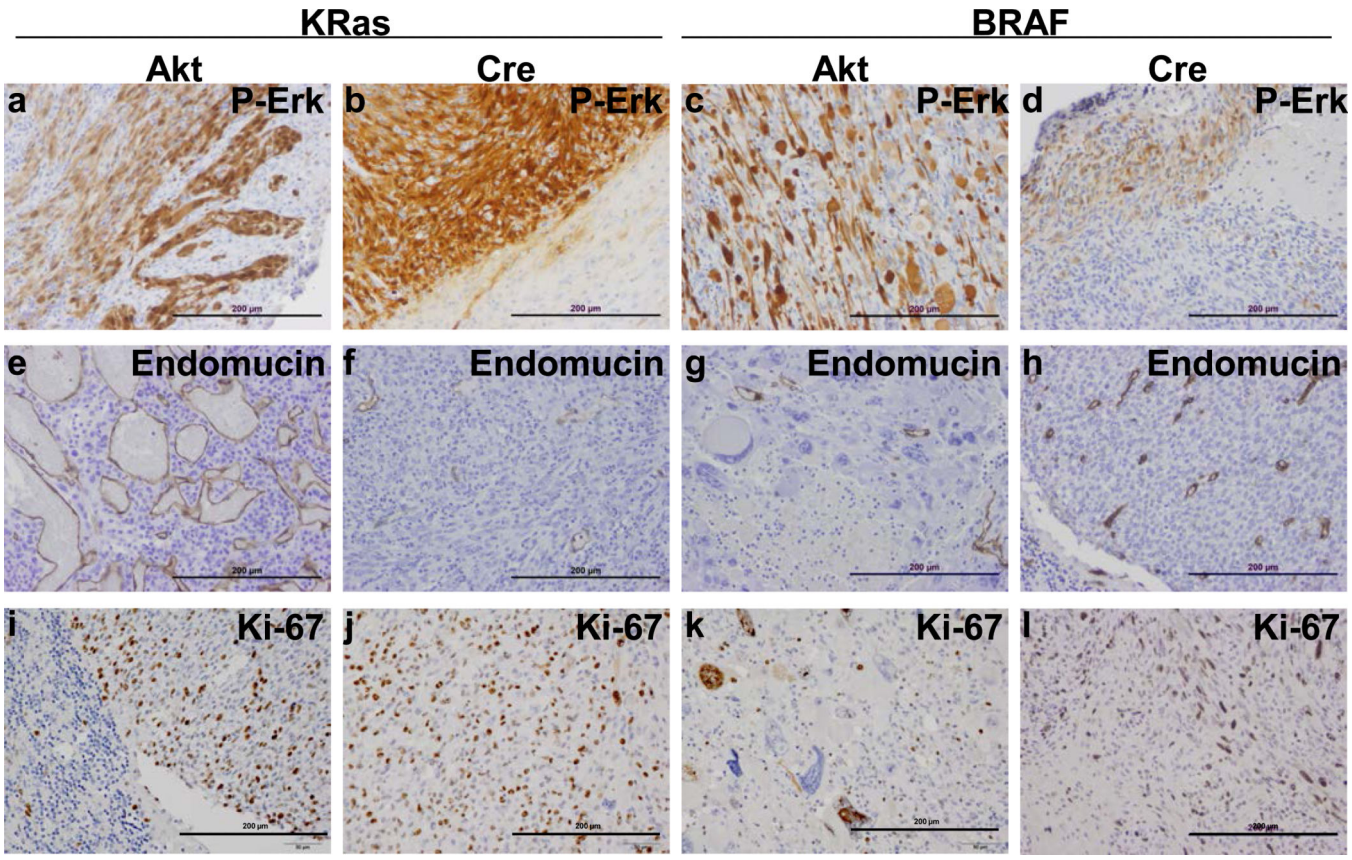

Figure 6. All gliomas demonstrate MAPK pathway activation and high levels of proliferation

(A-D) Confirmation of MAPK activation. IHC for P-Erk confirmed MAPK activation in all gliomas induced with either $KRas^{G12D}$ or $BRAF^{V600E}$. **(e-h)** Analysis of tumor vasculature. IHC for the endothelial cell marker endomucin highlights the highly abnormal vasculature of Akt/$KRas^{G12D}$ gliomas compared with the other tumor samples. **(i-l)** Assessment of mitotic activity. IHC for the cell division marker Ki67 demonstrates that all of the tumors are highly proliferative. Scale bars represent 200 μm.